Article No. jmbi.1999.3318 available online at http://www.idealibrary.com on IDEAL® J. Mol. Biol. (1999) 294, 1271–1285

JMB

X-ray Structure Determination of Human Profilin II: A Comparative Structural Analysis of Human Profilins

Ilana M. Nodelman[1], Gregory D. Bowman[1], Uno Lindberg[2] and Clarence E. Schutt[3]*

[1]*Department of Molecular Biology, Henry H. Hoyt Laboratory, Princeton University, Princeton NJ 08544, USA*

[2]*Department of Zoological Cell Biology, WGI, Arrhenius Laboratories for Natural Sciences, Stockholm University S-10691, Stockholm, Sweden*

[3]*Department of Chemistry Henry H. Hoyt Laboratory Princeton University Princeton NJ 08544, USA*

**Corresponding author*

Human profilins are multifunctional, single-domain proteins which directly link the actin microfilament system to a variety of signalling pathways *via* two spatially distinct binding sites. Profilin binds to monomeric actin in a 1:1 complex, catalyzes the exchange of the actin-bound nucleotide and regulates actin filament barbed end assembly. Like SH3 domains, profilin has a surface-exposed aromatic patch which binds to proline-rich peptides. Various multidomain proteins including members of the Ena/VASP and formin families localize profilin:actin complexes through profilin:poly-L-proline interactions to particular cytoskeletal locations (e.g. focal adhesions, cleavage furrows). Humans express a basic (I) and an acidic (II) isoform of profilin which exhibit different affinities for peptides and proteins rich in proline residues. Here, we report the crystallization and X-ray structure determination of human profilin II to 2.2 Å. This structure reveals an aromatic extension of the previously defined poly-L-proline binding site for profilin I. In contrast to serine 29 of profilin I, tyrosine 29 in profilin II is capable of forming an additional stacking interaction and a hydrogen bond with poly-L-proline which may account for the increased affinity of the second isoform for proline-rich peptides. Differential isoform specificity for proline-rich proteins may be attributed to the differences in charged and hydrophobic residues in and proximal to the poly-L-proline binding site. The actin-binding face remains nearly identical with the exception of five amino acid differences. These observations are important for the understanding of the functional and structural differences between these two classes of profilin isoforms.

Keywords: profilin; poly-L-proline; isoform; actin; cytoskeleton

Introduction

In eukaryotic cells there exists a complex web of signal transduction pathways which function to convey signals from cell surface receptors to the proper intracellular targets. The actin microfilament system is one of the major targets of signalling cascades whose activation is essential for fundamental cellular processes including motility (Stossel, 1993), endo- and exocytosis (Perrin *et al*., 1992), cytokinesis (Sanger *et al*., 1989) and determination of cell shape (Small, 1988). Profilin plays a central role by integrating multiple signalling pathways and directly affecting actin filament dynamics. *Via* profilin, actin is linked to the phosphoinositide cycle and to a host of pathways in which specific proline-rich proteins play a role.

Profilin is an essential protein (Verheyen & Cooley, 1994; Witke *et al*, 1993) which forms a 1:1 complex with monomeric actin. Profilin was first isolated from spleen and was thought to function as a sequesterer of monomeric actin (Carlsson *et al*., 1977); however, subsequent biochemical studies have shown its role to be more complex. In the presence of capped F-actin barbed ends, profilin acts as a sequesterer and causes the depolymerization of actin filaments (Pollard & Cooper, 1984;

Abbreviations used: Ena, enabled; VASP, vasodilator-stimulated phosphoprotein; N-WASP, neuronal Wiskott-Aldrich syndrome protein; WIP, WASP-interacting protein; DMSO, dimethyl sulfoxide; PIP_2, phosphatidylinositol 4,5-bisphosphate; PtdIns, phosphatidylinositol; PDB, Protein Data Bank; rms, root-mean-square; ATCC, American Type Culture Collection; NCS, non-crystallographic symmetry; PEG, polyethylene glycol; F-actin, filamentous actin.

E-mail address of the corresponding author: Schutt@chemvax.princeton.edu

0022-2836/99/501271–15 $30.00/0

Pantaloni & Carlier, 1993). In the absence of filament end cappers, profilin complexed to ATP-actin adds to the barbed ends of growing actin filaments (Pollard & Cooper, 1984; Pring *et al*., 1992; Pantaloni & Carlier, 1993; Korenbaum *et al*., 1998). Also, profilin catalyzes actin nucleotide exchange *in vitro*, thereby having the potential to increase the pool of ATP-actin necessary for barbed end assembly (Mockrin & Korn, 1980; Nishida, 1985; Goldschmidt-Clermont *et al*., 1991b). In agreement with its role as a key regulator of actin dynamics, profilin localizes to regions in the cell undergoing active cytoskeletal remodelling *in vivo* (Buss *et al*., 1992; Edamatsu *et al*., 1992; Finkel *et al*., 1994; Suetsugu *et al*, 1998; Wills *et al*, 1999).

Profilin binds to proline-rich stretches in a variety of proteins including members of the Ena/VASP (Reinhard *et al*., 1995; Gertler *et al*., 1996) and formin families (Manseau *et al*., 1996; Watanabe *et al*., 1997; Evangelista *et al*., 1997; Chang *et al*., 1997), drebrin (Mammato *et al*., 1998), gephyrin (Mammato *et al*., 1998), N-WASP (Suetsugu *et al*., 1998), WIP (Ramesh *et al*., 1997), dynamin I (Witke *et al*., 1998), and the p85 subunit of PI3-kinase (Singh *et al*., 1996). Members of the Ena/VASP family localize to focal adhesions and can interact with ActA on the surface of *Listeria monocytogenes*, a bacterial pathogen which utilizes actin to move through the cytoplasm (Chakraborty *et al*., 1995; Gertler *et al*., 1996). Cell polarization and cytokinesis require formin proteins and *via* their formin homology 1 domains associate with profilin (for a review, see Wasserman, 1998). Disruption of the *Drosophila* formin gene, *diaphanous*, results in defects in cytokinesis (Castrillon & Wasserman, 1994), and mutations in the human homologue of *diaphanous, DFNA1,* have been linked to an autosomal dominant hearing disorder (Lynch *et al*., 1997). Recruitment of profilin:actin complexes by these proline-rich ligands increases the local concentrations of actin necessary for the execution of various actin-driven processes.

Another way profilin links the cytoskeleton to signal transduction pathways is *via* a direct interaction with phosphoinositides. Phosphatidylinositol 4,5-bisphosphate (PIP_2) causes the dissociation of profilin:actin complexes *in vitro* which frees actin for rapid polymerization (Lassing & Lindberg, 1985). In addition, the PIP_2:profilin complex inhibits the hydrolysis of PIP_2 by phospholipase C-γ1 into second messengers (Goldschmidt-Clermont *et al*., 1990) which can be overcome by phosphorylation of the phospholipase (Goldschmidt-Clermont *et al*., 1991a). After several structural and mutagenic investigations (Raghunathan *et al*., 1992; Haarer *et al*., 1993; Fedorov *et al*., 1994a; Sohn *et al*., 1995) it still remains unclear if profilin has a distinct phosphoinositide binding site(s); yet, profilin binds phosphoinositides with varying affinities (PtdIns $(3,4)P_2$ > PtdIns$(3,4,5)P_3$ > PtdIns$(4,5)P_2$), suggesting some specificity of binding (Lu *et al*., 1996).

Mammals express two isoforms of profilin which are 62% identical in amino acid sequence. In 1993, human profilin II was cloned and shown to be expressed in different tissues than human profilin I, with profilin I apparently the more ubiquitously expressed of the two isoforms (Honoré *et al*., 1993). The relative affinities of profilin I and II for actin are comparable (Gieselmann *et al*., 1995; Lambrechts *et al*., 1995); however, opposing findings have been reported for the relative affinities of the profilin isoforms for PIP_2 (Gieselmann *et al*., 1995; Lambrechts *et al*., 1997). In contrast, differences between profilin I and II in their affinities towards poly-L-proline rich peptides (Lambrechts *et al*., 1997; Jonckheere *et al*., 1999) and proteins (Witke *et al*., 1998; Suetsugu *et al*., 1998) have been clearly established. Studies with continuous stretches of proline as well as VASP-based proline peptides have shown profilin II to bind more tightly than profilin I (Lambrechts *et al*., 1997; Jonckheere *et al*., 1999). Nevertheless, these peptide studies do not reflect the affinities of either isoform for proline-rich stretches presented in the context of a full-length protein. Recently, Suetsugu and co-workers showed profilin I to exhibit tighter binding to N-WASP compared with profilin II (Suetsugu *et al*., 1998), and studies by Witke and co-workers found that profilin I and II associated with different functional protein complexes from mouse brain extracts. In particular, profilin II was found to interact with dynamin I whereas profilin I did not (Witke *et al*., 1998). These data suggest that differences between the isoforms in and around the poly-L-proline binding site play a critical role in selecting different binding partners, which in turn link the actin cytoskeleton to distinct functional pathways.

The structure of profilins from human (Metzler *et al*., 1993; Mahoney *et al*., 1997; Mahoney *et al*., 1999), bovine (Schutt *et al*., 1993; Cedergren-Zeppezauer *et al*., 1994), *Saccharomyces cerevisiae* (Eads *et al*., 1998), *Acanthamoeba castellanii* (Vinson *et al*., 1993; Fedorov *et al*., 1994a), *Arabidopsis thaliana* (Thorn *et al*., 1997) and birch pollen (Fedorov *et al*., 1997) have previously been reported. Profilins have a common fold consisting of a central seven-stranded β-sheet flanked by N and C-terminal helices on one side and two short helices on the other side. X-ray structure determination of bovine profilin I in complex with bovine β-actin defined the actin binding site of profilin as residues from helix 3, helix 4, and β-strands 4, 5, and 6. Also, crystal structures of human profilin I bound to poly-L-proline peptides (Mahoney *et al*., 1997; Mahoney *et al*., 1999) have confirmed a previously described surface patch of aromatic residues (Trp3, Tyr6, Trp31, His133, Tyr139) as the poly-L-proline binding site (Björkegren *et al*., 1993; Schutt *et al*., 1993; Cedergren-Zeppezauer *et al*., 1994; Thorn *et al*., 1997). The uncomplexed structures of bovine profilin I and human profilin I are virtually identical with the actin- and poly-L-proline-complexed forms (Cedergren-Zeppezauer *et al*., 1994; Mahoney *et al*., 1997). Here, we pre-

sent the first X-ray crystal structure of this second class of mammalian profilins, human profilin II. This structure reveals an aromatic extension of the poly-L-proline binding site which may explain the increased affinity of profilin II for proline-rich peptides. Comparison with profilin I shows the region surrounding the poly-L-proline site to have a distinct electrostatic and hydrophobic character which may explain differential ligand specificities.

Results

Structure determination

The asymmetric unit of human profilin II consists of four molecules related by approximate 222 non-crystallographic symmetry (NCS) with the central interaction of the tetramer formed by all four C-terminal helices (Figure 1). Monomers related by the NCS 2-fold axis parallel to the crystallographic *c*-axis (A:C and B:D) interact at β-strands 4 and 5, the turn connecting β-strands 4 and 5, and the C-terminal helix of each molecule. The A:C and B:D interfaces each bury a total of 1171 $Å^2$ of solvent-accessible surface area. A second NCS 2-fold axis (roughly parallel with the crystallographic a-axis) relates A to B and C to D. The A:B interface includes contacts from the N and C-terminal helices burying a total of 966 $Å^2$ of solvent-accessible surface area. In contrast, a polyethylene glycol (PEG) 400 molecule is completely buried in the C:D interface which restricts direct contacts between chains C and D to include only the N-terminal residues. This PEG 400 molecule is stably bound with an average *B*-factor of 18.2 $Å^2$, and may account for the requirement of PEG 400 in the crystallization mixture.

Main-chain C^α atoms of A and B superimpose with an rms deviation of 0.26 Å while C and D C^α atoms superimpose with an rms deviation of 0.09 Å. C^α superposition of A or B onto C or D results in a slightly higher rms deviation of 0.47 Å. The first two amino acids are visible only in chains C and D, and the last two residues are disordered in all four chains. Also, the electron density is poor for residues 92-95 of the loop preceding β-strand 6 of chain B, whereas it is clearly defined for chains C and D. The presence of a second bound PEG 400 molecule and close packing contributes to differences in the local environments of this loop region in chains C and D. A sulfate molecule from the crystallization buffer is bound to each molecule in

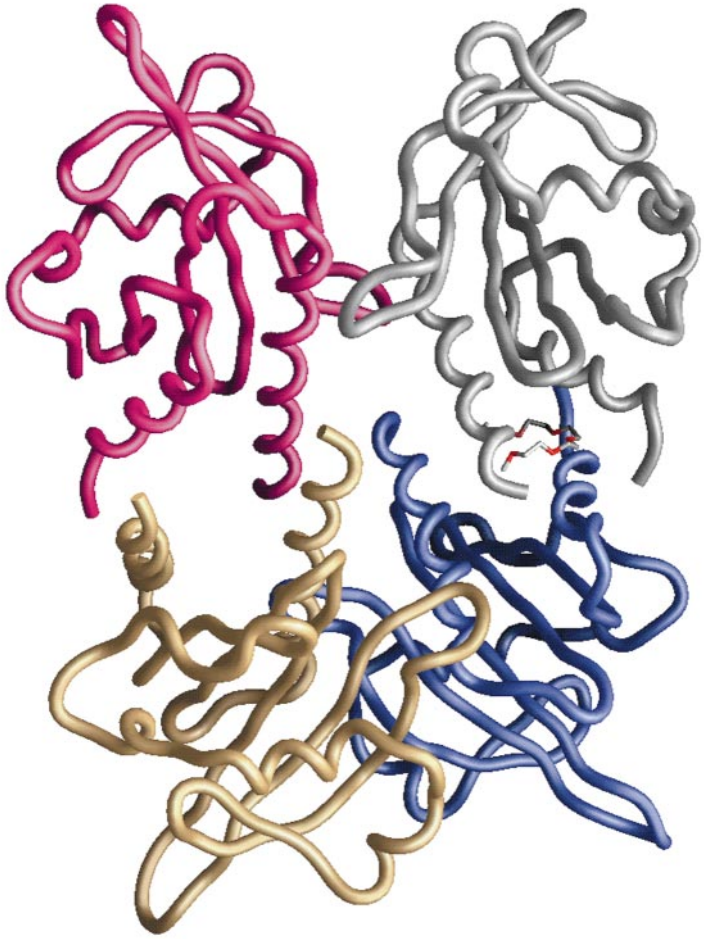

Figure 1. Backbone worm representation of the asymmetric unit in human profilin II crystals. The four chains, A, B, C, and D are colored pink, brown, gray, and blue, respectively. A PEG 400 molecule (red and gray sticks) is buried by the C:D interface.

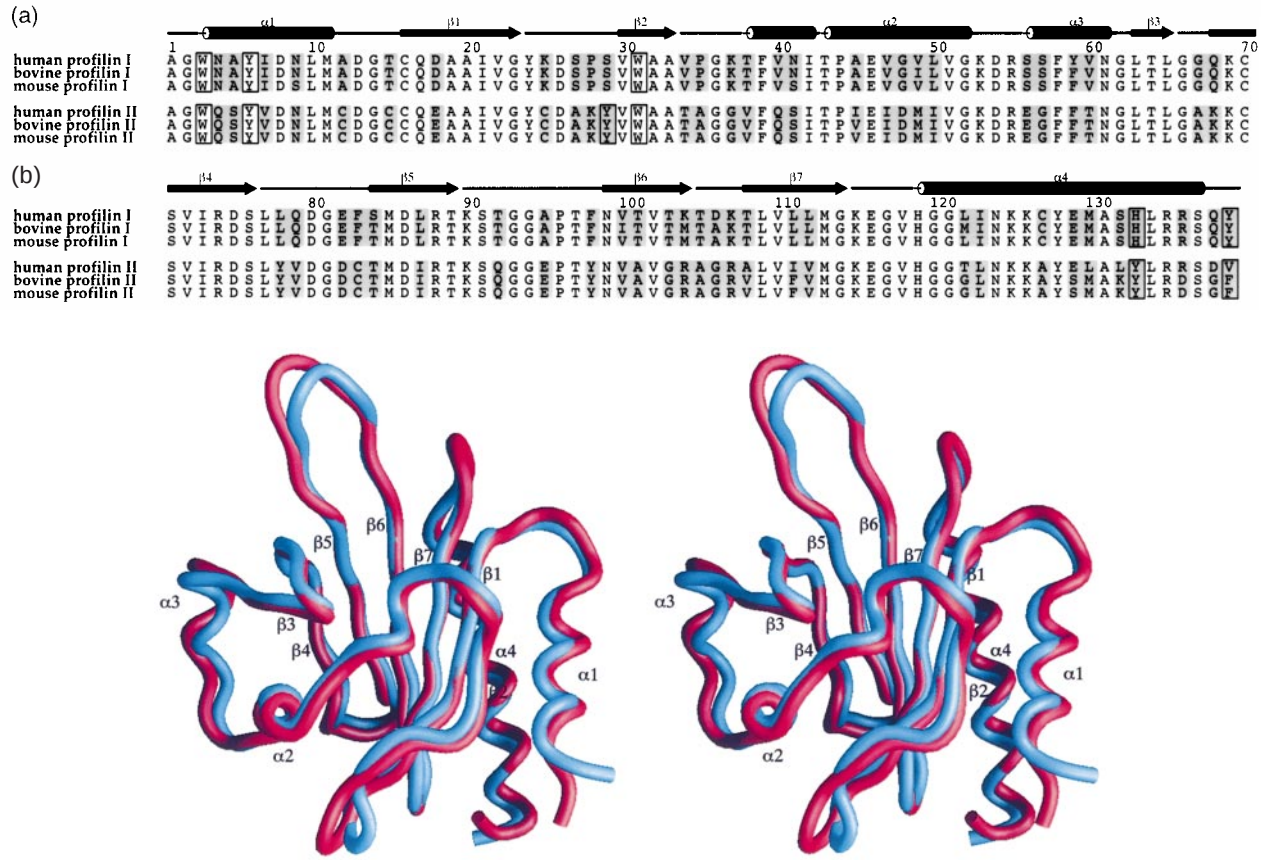

Figure 2. (a) Sequence alignment of mammalian profilins (human profilin I (Kwiatkowski & Bruns, 1988); human profilin II (Honoré *et al.*, 1993); bovine profilin I (Ampe *et al.*, 1988); bovine profilin II (Lambrechts *et al.*, 1995); mouse profilin I (Widada *et al.*, 1989); mouse profilin II (medline accession: AI322548)). Amino acid differences are shaded, and profilin I and putative profilin II poly-L-proline binding residues are boxed. Sequence alignment was generated using AMPS and ALSCRIPT (Barton *et al.*,1990; Barton *et al.*, 1993). (b) Superposition of human profilin I and II. Residues 3 to 136 of 1fik (red) were superimposed onto chain D of profilin II (blue). Secondary structural elements are labelled (α, alpha-helix; β, beta-strand).

the asymmetric unit, coordinated by the side-chains of Arg88, Asn99, His119, the main-chain amide group of Gly120 and the side-chain of Arg74 of a non-crystallographically related molecule. Similarly, two structures of human profilin I (PDB accession code: 1fik and 1fil; referenced in Materials and Methods) have a phosphate and a sulfate group positioned in the same location and coordinated by the same side-chains.

Structural overview of human profilins

Mammals express two isoforms of profilin in which each isoform class, I or II, is conserved between species. Human profilin I and II are 62% identical in primary sequence and share the same fold (Figure 2(a) and (b)). Residues 3 to 136 of human profilin I and II superimpose with an average C^{α} rms deviation of 1.13 Å (C^{α} atoms of chains A, B, C, and D were each superimposed onto crystal structures of human profilin I (PDB accession code: 1fik; 1fil; 1awi)). Slight deviations in the main chain are visible around loops preceding β-strands 2 and 6.

Based on sequence alignment, all amino acid differences between human profilin I and II which are solvent exposed (>10 $Å^2$ of solvent-accessible surface area) are highlighted on a surface rendering of human profilin II in Figure 3. These differences span most of the surface of the protein with the exception of the majority of the actin and poly-L-proline binding surfaces. A total of five amino acid differences, S56E, Y59F, V60T, E82D, and L122T (the first and second letters are the amino acids found at the given positions of human profilin I and II, respectively) are found in the actin-binding face. Residues surrounding the poly-L-proline binding site display a wide range of sequence variation which could result in differential binding specificities for proline-rich ligands.

The differences in sequence between the human profilin isoforms result in locally unique surface chemistry and topology without disruption of the profilin fold. Presumably, the presence of particu-

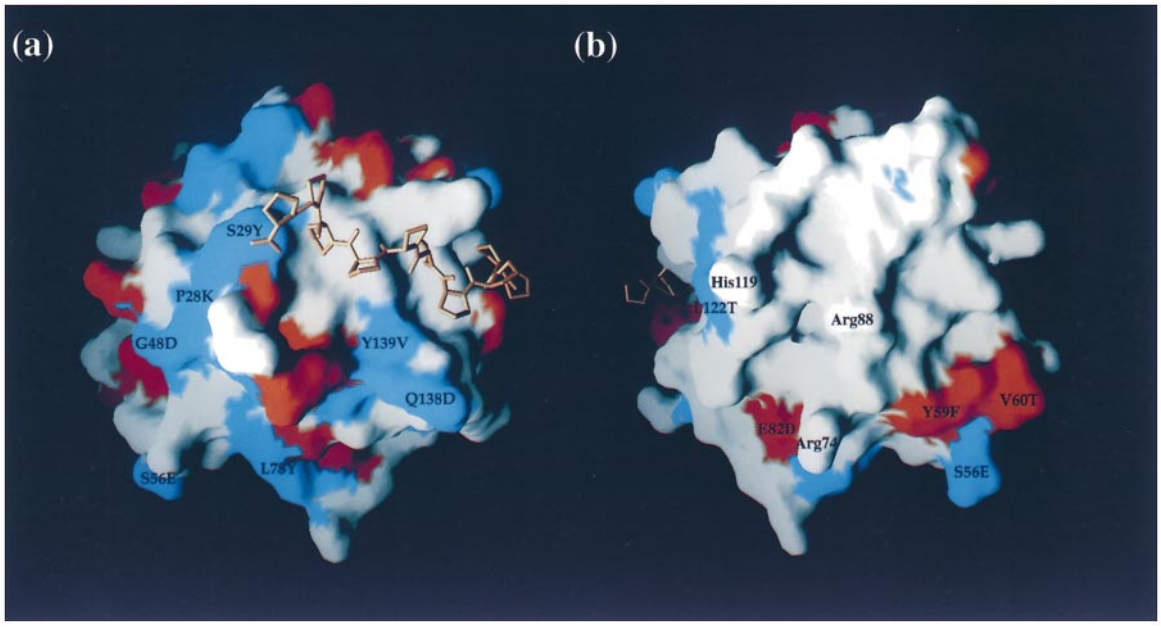

Figure 3. (a) and (b) Amino acid residue differences of the human profilins. A surface rendering of human profilin II (chain D) with colored regions highlighting amino acid residues which differ in human profilin I (blue, non-conserved amino acid changes; brown, conserved amino acid changes). Sites of the more dramatic differences are labelled, e.g. S29Y, with the first letter representing the amino acid in human profilin I followed by the residue number, ending with the amino acid present in human profilin II. Human profilin II was superimposed with human profilin I and bound proline peptide (PDB accession code: 1awi) to orient the poly-L-proline binding groove. Image (b) is rotated 180° about the *y*-axis with respect to (a). Image was generated using the program GRASP (Nicholls *et al.*, 1991).

lar intramolecular interactions are selectively maintained throughout evolution. For example, the second isoform of profilin has three cysteine residues (Cys12, Cys15, and Cys16) located on a structurally conserved loop following the N-terminal helix (Figure 4). Cys16 is conserved in profilin I and displays the same rotomer conformation as in profilin II. The sulfur atom of Cys15 (profilin II) is positioned similarly to the γ-oxygen atom of Thr15 (profilin I), and both form electrostatic interactions

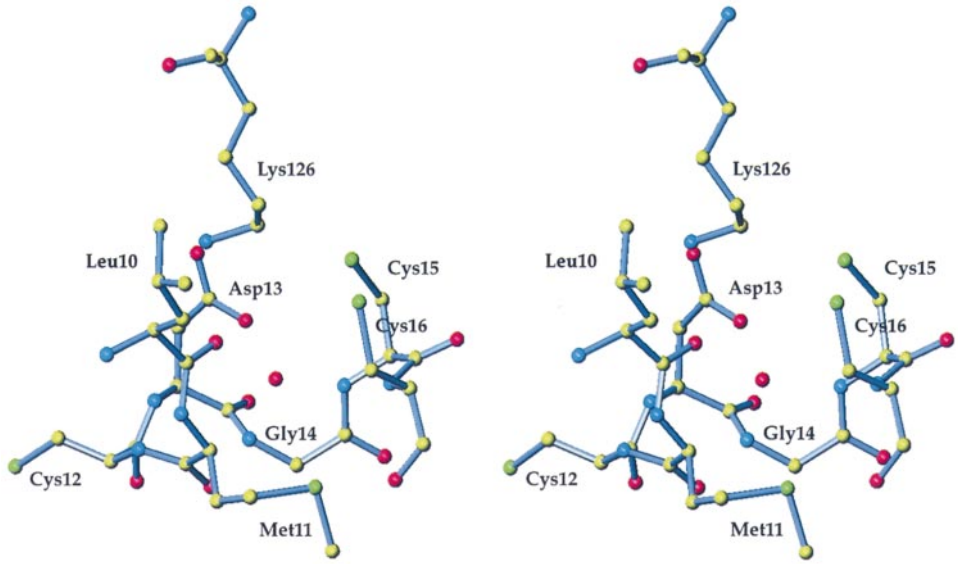

Figure 4. A cysteine-rich loop in human profilin II. Two additional cysteine residues are present in the loop proceeding the N-terminal helix in human profilin II compared with human profilin I. This loop also displays a conserved hydrogen-bonding network involving a water molecule in the human profilin isoforms (carbon, yellow; oxygen, red; nitrogen, blue; sulfur, green). The Figure was generated using the program O (Jones *et al.*, 1991).

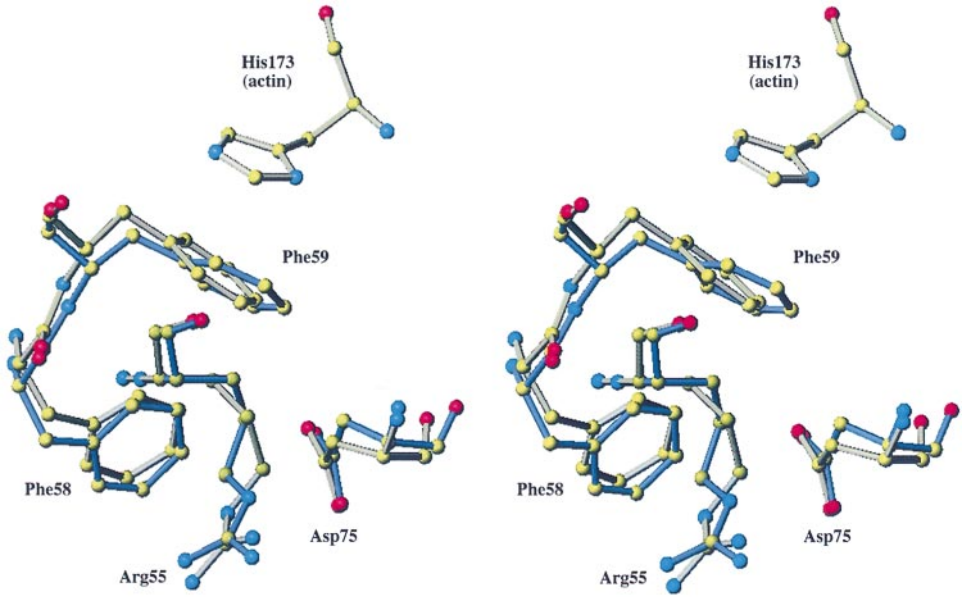

Figure 5. Stereo representation of structurally conserved interactions at the actin binding interface. Superposition of human profilin II (blue; chain D) onto bovine profilin I (gray) complexed to β-actin (PDB accession code: 2btf) illustrates the high degree of structural conservation of residues Phe59, Phe58, Arg55, and Asp75. His173 of β-actin stacks against Phe59 of bovine profilin I which in turn is stabilized by underlying aromatic and charged residues. The Figure was generated using the program O (Jones *et al*., 1991).

with the carboxylate group of Asp13. There is a conserved hydrogen-bonding network in and surrounding this loop which includes coordination of a water molecule by Asp13, the carbonyl oxygen atom of Leu10, and the backbone amides of residues 15 and 16. The side-chain of Asp13 also forms a hydrogen bond with the terminal amino group of Lys126, found on the second turn of the C-terminal helix. Additionally, Met11 extends from the final turn of helix 1 to pack against the base of this loop, which positions its δ-sulfur atom in proximity to the conserved loop.

Actin binding surface

In the X-ray structure of bovine profilin I complexed to β-actin, approximately 1050 Å^2 of the profilin I surface is excluded from solvent. Many profilin I residues which either directly interact with β-actin or act to position side-chains contacting actin are conserved in the profilin II isoform. Suetsugu *et al*. (1998) demonstrated dramatic loss of affinity for actin as a result of profilin His119 mutation to glutamic acid. In the profilin:β-actin complex, this histidine residue protrudes from the surface of profilin and sits in a pocket largely formed by Tyr133, Tyr169, Met355, and Phe375 of actin. Similar to His119, Phe59 contributes to the stabilization of the profilin:actin complex. Mutation of Phe59 to alanine results in the disruption of the π-stacking interaction with His173 of actin and a 14-fold decrease in affinity for actin (Schlüter *et al*., 1998). In contrast to His119, the rotomer conformation of Phe59 appears to be stabilized by three conserved residues in profilin (Figure 5). The aromatic ring of Phe59 participates in a T-shaped stacking arrangement (McGaughey *et al*., 1998) with Phe58 which in turn participates in an amino/aromatic interaction (Mitchell *et al*., 1994; Burley & Petsko, 1986) with the δ-guanido group of Arg55. This arginine is partially stabilized by an electrostatic interaction with the carboxylate oxygen atoms of Asp75.

The actin-binding face of bovine profilin I originally defined by Schutt *et al*. (1993) was used as the basis for comparing the putative actin binding sites of the human profilins. Overall, the actin-binding region of human profilin I is very similar to that of human profilin II with the exception of five amino acid differences. As seen in Figure 3(b), two notable differences are hydrophobic residues Val60 and Leu122 of human profilin I which are threonine in human profilin II. In the bovine profilin I:β-actin complex, the closest atom to the side-chain of Met122 of profilin is 5.42 Å away (C^{β} of Met122 to the ε-carbon atom of actin Lys373). The absence of side-chain contact and indifference to size at amino acid position 122 suggest that this residue contributes little to the stabilization of the profilin:actin complex. Val60 of bovine profilin I forms a more involved peripheral interfacial contact, packing against Val287 and Arg290 of actin. In human profilin II, the threonine residue at position 60 displays a similar rotomer conformation as that of bovine profilin I Val60. The substitution of a hydroxyl for a γ-methyl group at position 60 could allow for an additional hydrogen bond to the backbone carbonyl group of position 285 or the

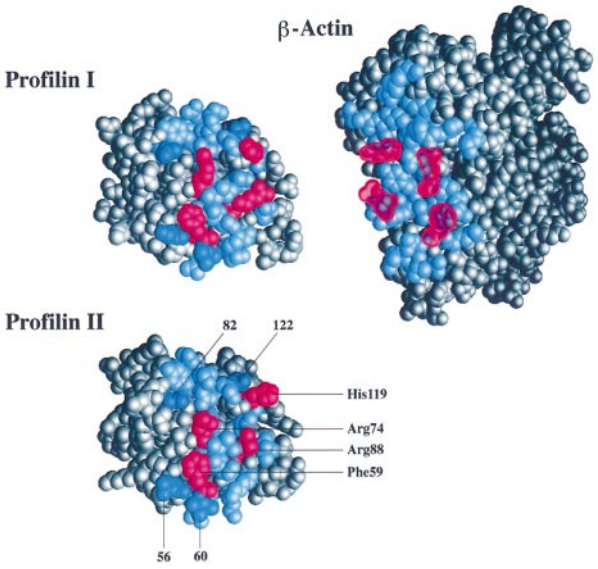

Figure 6. Conserved key residues and non-conserved isoform differences highlighted at the profilin:actin interface. The bovine profilin I:β-actin complex (top; 2btf) has been opened and rotated towards the observer to reveal the protein binding surfaces (light blue). Human profilin II (bottom) was superimposed onto bovine profilin I and translated. Residues colored red (Phe59, Arg74, Arg88 and His119) have been shown to contribute significantly to actin binding. The footprints of these residues are shown mapped onto β-actin as red transparent outlines. The differences between human profilin I and II at the actin-binding surface are colored dark blue (S56E, V60T, E82D, and L122T; first letter corresponds to profilin I, the second to profilin II). Although position 59 differs between human profilin I and II (Y59F) the essential character is conserved.

guanidium group of Arg290 of actin. Additionally, Cedergren-Zeppezauer *et al*. (1994) noted that the presence of glutamic acid in position 56 of profilin II (serine in profilin I) could result in the formation of a salt bridge to Lys284 of actin. The two final differences between human profilin I and II are conserved in character. Similar to Glu82 of bovine profilin I, the carboxylate group of Asp82 in profilin II would be expected to form a salt bridge with the amino-terminal group of Lys113 of actin. Amino acid position 59 is phenylalanine in all known mammalian profilin sequences, with the exception of human profilin I which encodes a tyrosine residue. The additional terminal hydroxyl group would not be capable of forming an intermolecular hydrogen bond with actin, and thus would not contribute an additional energy of binding.

It has been shown in the case of human growth hormone binding to its receptor that residues which make significant contributions in binding energy, known as ''hot spots'', are surrounded by residues which contribute little to binding energy (Clackson & Wells, 1995). Interestingly, all of the differences between human profilin I and II lie on the periphery of the actin binding surface (Figure 6). Residues at these positions would be expected to have little contribution to binding energy with the exception of the aromatic at position 59. Mutation of Phe59 to alanine ($K_d^{mutant} = 34$ μM, $K_d^{wild\text{-}type} = 2.3$ μM; Schlüter *et al*., 1998) corresponds to a binding energy of 1.53(±0.28) kcal/mol, or more than 16% of the total binding energy. Additionally, the amino acid identity, dramatic reduction in actin affinity upon mutagenesis (Sohn *et al*., 1995; Suetsugu *et al*., 1998; Korenbaum *et al*., 1998), and structural location in the profilin:actin interface of three conserved residues in mammalian profilins, Arg74, Arg88 and His119, suggest these residues are also key energetic contributors (Figure 6). In contrast, positions 56, 60, 82, and 122 may function in the exclusion of solvent from the key energetic interactions (Bogan & Thorn, 1998) due to their location in the actin-binding face, amino acid identity, and the comparable affinities of the human profilin isoforms towards actin.

Poly-L-proline binding site

As determined by site-directed mutagenesis and later confirmed by crystallographic studies, residues in profilin I which directly interact with stretches of poly-L-proline are Trp3, Tyr6, Trp31, His133, and Tyr139 (Björkegren *et al*., 1993; Mahoney *et al*., 1997; Mahoney *et al*., 1999). Superposition of human profilin II onto human profilin I complexed to a pentadeca-prolylpeptide (1cjf) allows for an analysis of the peptide:profilin II interactions (Figure 7(a)). Comparison of human profilin I poly-L-proline binding residues Trp3, Tyr6, Trp31, and His133 with the analogous positions in human profilin II reveals virtually identical rotomer conformations. In human profilin II, amino acid positions 133 and 139 are tyrosine and valine residues, respectively. Analogous to His133 of human profilin I, Tyr133 of human profilin II is capable of hydrogen bonding to the carbonyl oxygen atom of Pro11 and stacking against Pro13 of the pentadecapeptide (proline numbering according to 1cjf complex). Due to the disordering of the last two amino acids in human profilin II, backbone positioning of Val139 was modelled based on main-chain positioning of Tyr139 of human profilin I, showing Val139 positioned to make van der Waals contact with Pro10.

Due to the presence of tyrosine at position 29 in human profilin II, a slight shift in the proline pentadecamer was introduced in the first six proline residues to relieve minor clashes. The most striking feature of the pentadecamer modelled onto human profilin II is the evident extension of the aromatic region of the poly-L-proline binding site in human profilin II by Tyr29 (Figure 7(a)). This tyrosine residue protrudes from the surface of human profilin II and

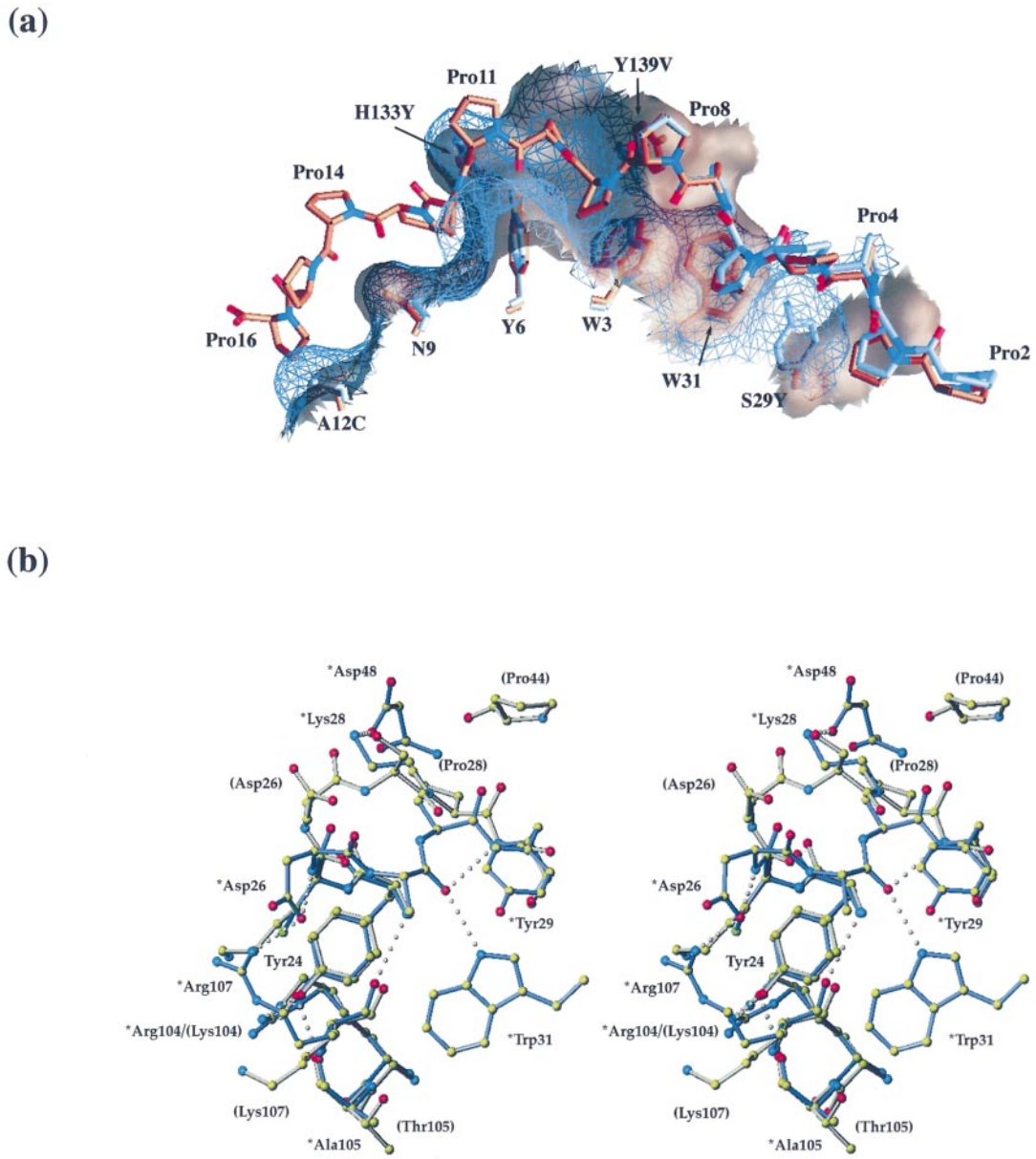

Figure 7. (a) Surface differences of the poly-L-proline binding site between the profilin isoforms. Human profilin II was superimposed onto human profilin I complexed to a proline pentadecamer (PDB accession code: 1cjf). Surface and bond coloring corresponds to human profilin I (brown) and II (blue). Residues comprising the poly-L-proline binding site are illustrated as rods and labelled as in Figure 3. The prolylpeptide complexed to human profilin I (brown) was modelled (blue) to alleviate minor clashes with the protruding Tyr29 residue of human profilin II. The protein surfaces within 4 Å of the respective prolylpeptide are displayed in transparent (profilin I) and mesh (profilin II) renderings. The Figure was generated using the program GRASP (Nicholls *et al.*, 1991). (b) Architectural differences between the human profilin isoforms in or proximal to the poly-L-proline binding site. Stereo ball-and-stick representation of human profilin I (gray; PDB accession code: 1awi) superimposed with human profilin II (blue; chain D). Residue labels are marked with an asterisk * or parentheses () to indicate profilin I or II, respectively. Small spheres represent hydrogen bonds illustrated for profilin II only. The Figure was generated using O (Jones *et al.*, 1991).

accommodates an additional turn of the poly-L-proline helix. Tyr29 has the potential to form a stacking interaction with Pro3 and a hydrogen bond with the carbonyl group of Pro4, whereas position 29 in profilin I is a serine residue which makes van der Waals contacts to Pro3. Another unexpected difference occurs at amino acid position 12. Cys12 of profilin II is capable of contributing a larger surface area to interact with Pro16 than Ala12 of profilin I (Figure 7(a)).

Isoform-specific interactions contribute to variations in the local architecture of the loop contain-

ing residue 29 (Figure 7(b)). Two charged residues unique to the profilin II isoform, Lys28 and Asp48, participate in an electrostatic interaction in which the amino group of Lys28 forms a hydrogen bond with the carboxylate group of Asp48, a residue on helix 2. Profilin I has proline in amino acid position 28 which forms a van der Waals interaction with Pro44 of helix 2. A second stabilizing interaction in profilin II is formed between the carboxylate group of Asp26 which participates in an electrostatic interaction with the guanidinium group of Arg107, a residue found on the β-turn preceding β-strand 7. Although the charges at position 26 and 107 are conserved in both human profilin isoforms, they do not form an electrostatic interaction in any of the structures of human profilin I (1fik, 1fil, 1awi and 1cjf). Instead, the terminal amino group of Lys25 forms a weak salt bridge (4.2 Å) to the carbonyl oxygen atom of Asp106 (not illustrated in Figure 7(b)). In addition, the positioning of the backbone in human profilin II places the carbonyl oxygen atom of Ala27 within hydrogen bonding distance of the indole nitrogen atom of Trp31. Furthermore, the carbonyl oxygen atom of Ala27 hydrogen bonds with the backbone amide of Tyr29 forming an i to $i+2$ hydrogen bond characteristic of γ-turns. Residues 27 to 29 of human profilin II form an inverse γ-turn with a negative φ value for the $(i+1)$ position, whereas residues 25-27 of human profilin I form a classic γ-turn with a positive phi value for the $(i+1)$ position (Milner-White *et al.*, 1988). The positioning of this loop region in profilin II may be important for presentation of Tyr29 in a spatial context competent for binding to poly-L-proline.

It has been shown that hydrophobicity plays an important role in protein:protein interactions (Janin & Chothia, 1978). A hydrophobic patch on bovine profilin I has been previously described which is separated by a polar strip of residues from the poly-L-proline binding site and defined by residues: Tyr24, Pro28, Pro44, Val51, Leu78, Phe83, Met104, Ala106, and Tyr128 (Cedergren-Zeppezauer *et al.*, 1994). Residues comprising this hydrophobic patch are largely conserved between bovine and human profilin I, with the exception of positions 104 and 106. This region in human profilin II is less conserved and does not form a contiguous hydrophobic patch. In contrast with the patch described for bovine profilin I, human profilin II has a surface-exposed hydrophobic region which is contiguous with the poly-L-proline binding site. This hydrophobic area, neighboring Tyr29, is made up of side-chains from Pro44, Ile45, Met49, the C^{δ} of Thr43 and the aliphatic portion of Lys28 (Figure 8). The large aliphatic side-chains of Ile45 and Met49 protrude from the surface in human profilin II in contrast to the smaller side-chains of Ala45 and Val49 in human profilin I. These aliphatic regions near the poly-L-proline binding site may contribute to differences in ligand specificity.

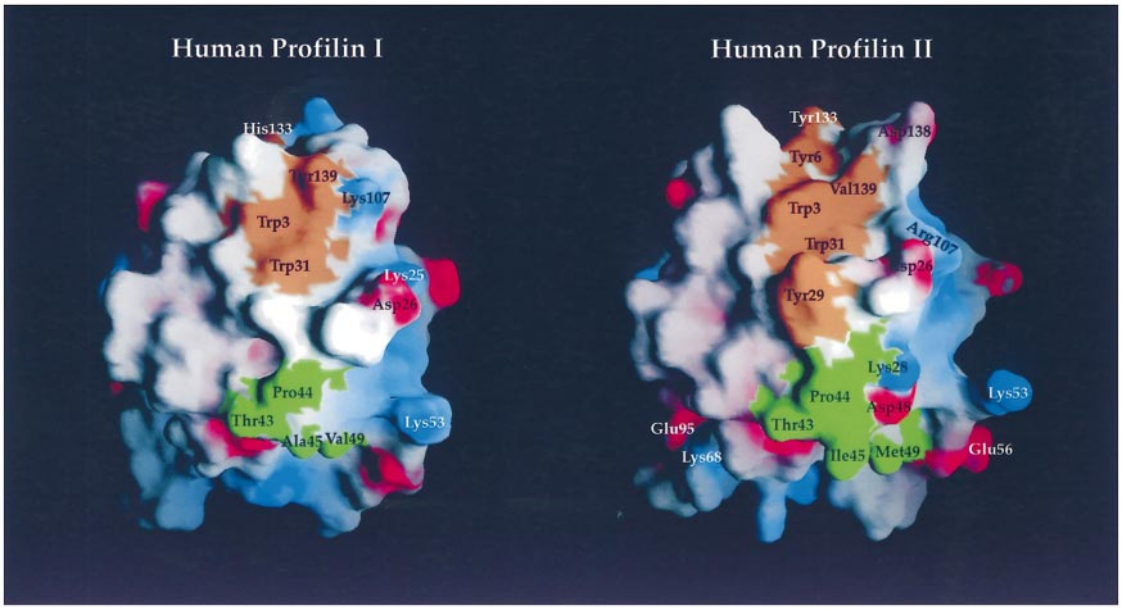

Figure 8. Charge and hydrophobic differences between human profilin I and II surrounding the poly-L-proline binding site. Electrostatic surface potentials of human profilin I (PDB accession code: 1fik) and II (chain D) were generated using GRASP (Nicholls *et al.*, 1991). The brown patch represents side-chains of poly-L-proline binding residues in human profilin I and analogous residues in human profilin II were colored brown and mapped to the surface. Also, the surface area of a flanking hydrophobic region differs between the two human isoforms (only side-chains are colored green and then mapped to the surface). The proteins are displayed in the same orientation. All visible charged residues which differ between the profilin isoforms have been labelled.

Acidic *versus* basic character of the human profilins

Human profilin I and II are often noted for their basic and acidic isoelectric points, respectively (Honoré *et al*., 1993). Human profilin II has four acidic residues (Asp48, Glu56, Glu95, Asp138) and two basic residues (Lys28 and Lys68) which are not found in human profilin I. Likewise, human profilin I has four charged residues (Lys25, Lys37, Asp106, His133) which are not conserved in human profilin II. The majority of these non-conserved differences between the two isoforms are located in (Asp138-II, His133-I) or proximal to (Lys25-I, Lys28-II, Asp48-II, Asp106-I) the poly-L-proline peptide binding site. The location of these charge differences suggests these residues might contribute to the differential affinities displayed by the profilin isoforms for poly-L-proline-rich proteins (Figure 8).

The two basic residues found in profilin II, but not in profilin I, participate in electrostatic interactions with two of the four acidic residues unique to profilin II. Lys28, on the loop between β-strands 6 and 7, forms a hydrogen bond with Asp48 which resides on helix 3 (Figure 7(b)). A second pairwise hydrogen-bonding interaction occurs between Glu95 of β-strand 6 and Lys68 of β-strand 4. The remaining two non-conserved acidic residues in profilin II are Glu56 and Asp138. Glu56 is fully exposed and does not participate in any intramolecular electrostatic interactions. The position of Asp138 can only be approximated in human profilin II due to poor electron density. A molecular surface rendering of human profilin II indicates that Asp138 is situated adjacent to an acidic position unique to human profilin I (Asp106), suggesting that the localized acidic character has shifted slightly between isoforms. Similarly, each of the basic residues specific to human profilin II (Lys28, Lys68) is spatially proximal to the position of a basic residue found only in profilin I (Lys25, Lys37).

Discussion

The structure determination of human profilin II has allowed for a comparative analysis of the two human profilin isoforms. Amino acid differences between the isoforms are seen throughout the surface of the protein with the exception of the majority of the actin and poly-L-proline binding faces. These differences contribute to locally unique chemical environments and topologies, which form the structural basis for functional distinctions between profilin I and II.

Mammalian profilin II isoforms display a higher affinity for proline-rich peptides than profilin I (Lambrechts *et al*., 1997; Jonckheere *et al*., 1999). Binding experiments of profilin I and II to a VASP-based peptide containing the $(GP_5)_3$ repeat demonstrated that bovine profilin II bound the VASP peptide with a dissociation constant of 0.5μM whereas profilin I bound with a K_d value of 150 μM (Jonckheere *et al*., 1999). Elution of profilin II from poly-L-proline Sepharose requires higher DMSO (this study; see Materials and Methods) or urea (Lambrechts *et al*., 1995) concentrations than profilin I, also indicating that profilin II has a tighter association with proline-rich stretches. The higher affinity of profilin II for proline-rich peptides may be attributed to the aromatic extension of the poly-L-proline binding site by tyrosine 29. The presence of tyrosine at this position, in lieu of serine as found in profilin I, may further stabilize a bound proline stretch through hydrogen bonding and accommodating an additional turn of the poly-L-proline type II helix *via* stacking and van der Waals interactions.

Other profilin surface features proximal to the ''core'' poly-L-proline binding site need to be considered when the proline stretch is presented in the context of a folded domain. Suetsugu and co-workers recently demonstrated profilin I binds one order of magnitude ($K_d = 60$ nM) more tightly to N-WASP over profilin II ($K_d = 400$ nM; Suetsugu *et al*., 1998). Notably, the proline-rich region of N-WASP harbors several of the (GP_5) repeats albeit not consecutively as in VASP. The discrepancy between the tighter binding of profilin II to $(GP_5)_3$ and the higher affinity of profilin I to full-length N-WASP strongly suggests that regions flanking the poly-L-proline binding site are important for these differences in specificity. As was shown in the case of the SH3 domains, the unusually tight binding of HIV-1 nef protein to the SH3 domain of hck is due to a region outside the aromatic poly-L-proline binding site. A region on the hck SH3 domain known as the RT loop contains isoleucine in position 96 which is critical for tight binding to HIV-1 nef protein (Lee *et al*., 1995). A crystal structure complex of the conserved core of HIV-1 nef protein bound to a high affinity mutant of fyn SH3 domain (Arg96 → Ile) shows the critical region of binding to be located outside of the poly-L-proline binding site and increases the solvent-excluded surface area from 780 Å^2 (poly-L-proline peptide binding region only) to 1200 Å^2 (Lee *et al*., 1996; Lim, 1996). Comparative structural analysis of the human profilin isoforms shows that six out of ten charged differences are in or proximal to the poly-L-proline binding face. Although the precise elements of structural specificity cannot be addressed without mutagenesis and/or structural studies of the particular profilin:ligand complex, the differences bordering the poly-L-proline binding site may play a critical role in recognition of the region surrounding the proline-rich target.

It has been shown that a fraction of residues in a protein:protein interface contribute the majority of the binding energy (Cunningham & Wells, 1993; Clackson & Wells, 1995; Bogan & Thorn, 1998). These key residues, referred to as hot spots, are

often located near the center of the interface and are most often tryptophan, arginine, or tyrosine residues. In contrast, residues which lie on the periphery of the interface typically make insignificant contributions to binding energy, and are thought to function primarily in the exclusion of solvent (for a review, see Bogan & Thorn, 1998). With respect to the profilin:actin interaction, both profilin isoforms show comparable affinity to actin which is consistent with the maintenance of key actin binding residues and the location and nature of the amino acid differences between isoforms (Figure 6). Although systematic alanine-scanning of the actin binding surface of profilin along with the respective dissociation constants has not been reported, mutagenesis studies of Phe59 (Schlüter *et al*., 1998), Arg74 (Korenbaum *et al*., 1998), Arg88 (Sohn *et al*., 1995) and His119 (Suetsugu *et al*., 1998) show dramatic effects on actin affinity, and suggest that these residues may be hot spots. The peripheral differences between the human profilin isoforms (positions 56, 60, 82, and 122) may result in kinetic differences in the association rates of profilin I and II with actin, as was seen in the case of human growth hormone and its receptor that peripheral electrostatic residues function to increase the rate of association (Cunningham & Wells, 1993).

The binding of PIP_2 to either of the mammalian profilin isoforms disrupts the profilin:actin complex, however there is disagreement as to the relative affinities of each isoform for polyphosphoinositides (Gieselmann *et al*., 1995; Lambrechts *et al*., 1997). It has been suggested that profilin is capable of associating with several PIP_2 molecules *via* profilin's positive electrostatic surface potential (Goldschmidt-Clermont *et al*., 1990; Fedorov *et al*., 1994a). There are ten charged differences between human profilin I and II and structural comparison shows that many of these differences are spatially close to the position of the charged residue in the other isoform (Asp138-II and Asp106-I; Lys28-II and Lys25-I; Lys68-II and Lys37-I) such that on a global scale the human profilin isoforms appear to share the same electrostatic patterns. Similar to *Acanthamoeba* profilin I and II (Fedorov *et al*., 1994a), the electrostatic surface of each of the two human isoforms presents two large basic patches that are separated by a common border of acidic residues (data not shown). Mutagenesis of single amino acids has been carried out to locate residues critical for PIP_2 interaction (Haarer *et al*., 1993; Sohn *et al*., 1995), yet none abolish binding. Mutation of Arg88 to leucine in human profilin I results in a threefold decrease in PIP_2 binding (Sohn *et al*., 1995). Interestingly, in three of the human profilin crystal structures (1fik, 1fil, and here), a negatively charged phosphate or sulfate anion is bound to a basic pocket consisting of Arg88, Asn99, His119 and the mainchain amide of residue 120. Notably, 1fik was solved in low salt, 30% PEG 8000 and 50 mM potassium phosphate (Fedorov *et al*., 1994b), which would correspond to a 1:100 ratio of profilin I to phosphate. The general propensity of profilin to accommodate a negatively charged group in this pocket lends support to the idea that these residues participate in phophoinositide binding.

Overall, profilin isoforms from many different species share the same global biochemical characteristics even with a considerable degree of sequence variation. The two human isoforms have a higher level of sequence similarity, and yet differences on the atomic level reflect the distinct signalling and biochemical pathways specific to the tissues in which each isoform is expressed. The finding that profilin I and profilin II associate with different functional complexes from brain lysates indicates that these isoforms have distinct roles in tissues where they are coexpressed (Witke *et al*., 1998). Sequence variation between profilin I and II also suggests the ability to bind to proline-rich ligands is differentially regulated by phosphorylation. Profilin I is phosphorylated on Tyr139 in an EGF-stimulated assay which leads to the inability to bind to poly-L-proline (Björkegren-Sjögren *et al*., 1997); whereas profilin II encodes a valine or phenylalanine residue in position 139. An atomic resolution structure of profilin in complex with a full-length proline-rich protein will be necessary to elucidate the structural determinants not evident in the structural studies of profilin:peptide complexes. The comparative analysis presented here will aid characterization of the profilin:ligand interface with respect to isoform specificity, and may provide insight into the basis for two distinct profilin isoforms.

Materials and Methods

Expression and purification of human profilin II

The cDNA for human profilin II was obtained from ATCC #84635, subcloned into a pET/T7 plasmid (Novagen) and transformed into *Escherichia coli* strain BL21(DE3). Low protein expression due to two unpreferred arginine codons was boosted using an ArgU plasmid (courtesy of Professor J. Walker), resulting in approximately 20 mg of protein from a ten liter fermentor growth. Human profilin II was purified according to Lindberg *et al*. (1988) with modifications. Briefly, the freeze-thaw technique (Johnson & Hecht, 1994) was used to extract human profilin II without cell lysis into the poly-L-proline Sepharose loading buffer A (10 mM Tris-HCl (pH 8.0), 100 mM KCl, 100 mM glycine). The purification was performed in batch and human profilin II was eluted from the poly-L-proline Sepharose in several washes of buffer A with 50% DMSO in contrast to 30% for the profilin I isoforms. Protein was dialyzed into 15 mM Tris (pH 7.5), 50 mM KCl under nitrogen and concentrated by ultrafiltration to 30 mg/ml. Human profilin II was passed over an S-100 column (Pharmacia), desalted using a PD-10 column (Pharmacia) into 15 mM Tris-HCl (pH 7.5), 10 mM DTT and concentrated by ultrafiltration (Amicon/centricon) to 18 mg/ml. Protein purity was monitored by silver and Coomassie stain as

Table 1. Data collection and statistics

A. *Data set*	
Space group	$P2_1$
Cell dimensions (Å; deg.)	$a = 71.43$
	$b = 44.80$
	$c = 89.60$
	$\beta = 98.59$
Molecules per asymmetric unit	4
Solvent content (%)	56
Resolution (Å)	50-2.2
No. of reflections	
Observed	430,124
Unique	28,050
$\langle I/\sigma(I)\rangle$	10.3
Completeness (%)	
Overall	96.9
Highest shell	83.5
R_{merge} [a] (%)	8.9
B. *Refinement statistics*	
Resolution (Å)	20-2.2
R_{cryst} [b] (%)	21.51
R_{free} [c] (%)	26.78
No. of water molecules	398
Average *B*-factor (Å^2)	
All atoms	23.00
Overall (protein)	17.57
Main-chain	17.40
Side-chain	17.78
Water molecules	27.82
rms deviations from ideality	
Bonds (Å)	0.007
Angles (deg.)	1.34

[a] $R_{merge} = \Sigma|I - \langle I\rangle|/\Sigma I$, where $\langle I\rangle$ is the average of symmetry-equivalent reflections and the summation extends over all observations for all unique reflections.

[b] $R_{cryst} = \Sigma||F_o| - |F_c||/\Sigma|F_o|$, where F_o and F_c are the observed and calculated amplitudes.

[c] R_{free} set contains 5.3 % of total reflections.

well as electrospray mass spectroscopy which showed a molecular mass corresponding to human profilin II lacking an amino-terminal methionine residue. This recombinantly expressed profilin lacked the N-terminal acetylation commonly observed on profilins purified from mammalian tissue. Protein concentration was measured using an extinction coefficient of 1.4 at 280 nm.

Crystallization and data collection

Human profilin II crystals grew in hanging drops consisting of 2 µl of protein solution mixed 1:1 with and equilibrated against a well solution of 1.35 M $MgSO_4$, 1.5 % (v/v) PEG 400, 100 mM Hepes (pH 7.3) at 4 °C. Crystals were bathed in increasing concentrations of ethylene glycol plus mother liquor and flash frozen at a final concentration of 12 % (v/v) ethylene glycol. Data were collected at 100 K at Brookhaven National Laboratories on beamline X9B. Human profilin II crystallized in the space group $P2_1$ with four molecules in the asymmetric unit. Data reduction and scaling were performed using DENZO/HKL suite (Otwinowski & Minor, 1997; see Table 1).

Structure determination

Bovine profilin I (PDB accession code 1pne) was employed as a molecular replacement search model, with all non-conserved residues modified to alanine. Molecular replacement solutions for all four molecules in the asymmetric unit were determined using AMoRe (Navaza, 1994) as part of the CCP4 suite of programs (Collaborative Computational Project, 1994). The ASU is a dimer of dimers with roughly 222 NCS symmetry. Cycles of building and refinement were performed using O (Jones *et al*., 1991) and XPLOR with bulk solvent correction (Brünger, 1993). During the first cycles of refinement NCS restraints grouped all four molecules. In later stages NCS restraints grouped A to B and C to D, and in the final rounds of refinement all NCS restraints were lifted. Solvent molecules were added to stereochemically sensible positions and a sulfate group was placed in identical positions for each of the four chains. Also, two PEG 400 molecules of varying length were modelled as described in the text.

Analysis

Structures of mammalian profilin I used in structural comparisons with human profilin II were: PDB accession code 1fik (human profilin I crystallized in low salt; Fedorov, A.A., Pollard, T.D., Almo, S.C.), 1fil (human profilin I crystallized in high salt; Fedorov, A.A., Pollard, T.D., Almo, S.C.), 1cjf (Mahoney *et al*., 1999), 1awi (Mahoney *et al*., 1997), 1pne (Cedergren-Zeppezauer *et al*., 1994), and 2btf (Schutt *et al*., 1993). All solvent-accessible surface area calculations were performed using GRASP with a probe radius of 1.4 Å (Nicholls *et al*., 1991). Protein secondary structure was analyzed using PROMOTIF (Hutchinson & Thornton, 1996) and protein superpositions were performed using O (Jones *et al*., 1991).

Coordinates

The coordinates and experimental amplitudes have been deposited in the Protein Data Bank (PDB accession code 1D1J).

Acknowledgments

We are indebted to Kevin Parris for his crystallographic advice and support. We thank Robert Sweet for organizing DataCol99, the workshop in which this dataset was collected, and Zbigniew Dauter for assistance on beamline X9B. We are grateful to Elspeth Garman for technical advice and to Herwig Schüler for critical comments on the manuscript. We thank Professor J. Walker for the use of the ArgU plasmid for protein expression. I.M.N. was supported by an NIH pre-doctoral training grant in molecular biophysics (GM08309). G.D.B. and C.E.S. were supported by grants from the National Institutes of Health (GM44038) and U.L. from the Swedish Cancer Foundation and the Swedish Natural Science Research Council.

References

Ampe, C., Markey, F., Lindberg, U. & Vandekerckhove, J. (1988). The primary structure of human platelet

profilin: reinvestigation of the calf spleen profilin sequence. *FEBS Letters,* **228**, 17-21.

Barton, G. J. (1990). An efficient algorithm to locate all locally optimal alignments between two sequences allowing for gaps. *Comput. Appl. Biosci.* **9**, 729-734.

Barton, G. J. & Sternberg, M. J. (1993). Flexible protein sequence patterns. A sensitive method to detect weak structural similarities. *J. Mol. Biol.* **212**, 389-402.

Björkegren, C., Rozycki, M., Schutt, C. E., Lindberg, U. & Karlsson, R. (1993). Mutagenesis of human profilin locates its poly(L-proline)-binding site to a hydrophobic patch of aromatic amino acids. *FEBS Letters,* **333**, 123-126.

Björkegren-Sjögren, C., Korenbaum, E., Nordberg, P., Lindberg, U. & Karlsson, R. (1997). Isolation and characterization of two mutants of human profilin I that do not bind to poly(L-proline). *FEBS Letters,* **418**, 258-264.

Bogan, A. A. & Thorn, K. S. (1998). Anatomy of hot spots in protein interfaces. *J. Mol. Biol.* **280**, 1-9.

Brünger, A. T. (1993). *XPLOR Version 3.1. A System for X-ray Crystallography and NMR*, Yale University Press, New Haven.

Burley, S. K. & Petsko, G. A. (1986). Amino-aromatic interactions in proteins. *FEBS Letters,* **203**, 139-143.

Buss, F., Temm-Grove, C., Henning, S. & Jockusch, B. M. (1992). Distribution of profilin in fibroblasts correlates with the presence of highly dynamic actin filaments. *Cell Motil. Cytoskel.* **22**, 51-61.

Carlsson, L., Nyström, L.-E., Sundkvist, I., Markey, F. & Lindberg, U. (1977). Actin polymerization is influenced by profilin, a low molecular weight protein in non-muscle cells. *J. Mol. Biol.* **115**, 465-483.

Castrillon, D. H. & Wasserman, S. A. (1994). *diaphanous* is required for cytokinesis in *Drosophila* and shares domains of similarity with the products of the *limb* deformity gene. *Development,* **120**, 3367-3377.

Cedergren-Zeppezauer, E. S., Goonesekere, N. C. W., Rozycki, M. D., Myslik, J. C., Dauter, Z., Lindberg, U. & Schutt, C. E. (1994). Crystallization and structure determination of bovine profilin at 2.0 Å resolution. *J. Mol. Biol.* **240**, 459-475.

Chakraborty, T., Ebel, F., Domann, E., Niebuhr, K., Gerstel, B., Pistor, S., Temm-Grove, C. J., Jockusch, B. M., Reinhard, M., Walter, U. & Wehland, J. (1995). A focal adhesion factor directly linking intracellularly motile *Listeria monocytogenes* and *Listeria ivanovii* to the actin-based cytoskeleton of mammalian cells. *EMBO J.* **14**, 1314-1321.

Chang, F., Drubin, D. & Nurse, P. (1997). cdc12p, a protein required for cytokinesis in fission yeast is a component of the cell division ring and interacts with profilin. *Cell Biol.* **137**, 169-182.

Clackson, T. & Wells, J. A. (1995). A hot spot of binding energy in a hormone-receptor interface. *Science,* **267**, 383-386.

Collaborative Computational Project Number 4 (1994). The *CCP4* suite: programs for protein crystallography. *Acta Crystallog. sect. D,* **50**, 760-763.

Cunningham, B. C. & Wells, J. A. (1993). Comparison of a structural and functional epitope. *J. Mol. Biol.* **234**, 554-563.

Eads, J. C., Mahoney, N. M., Vorobiev, S., Bresnick, A. R., Wen, K.-K., Rubenstein, P. A., Haarer, B. K. & Almo, S. C. (1998). Structure determination and characterization of *Saccharomyces cerevisiae* profilin. *Biochemistry,* **37**, 11171-11181.

Edamatsu, M., Hirono, M. & Wanatabe, Y. (1992). *Tetrahymena* profilin is localized in the division furrow. *Biochemistry,* **112**, 637-642.

Evangelista, M., Blundell, K., Longtine, M. S., Chow, C. J., Adames, N., Pringle, J. R., Peter, M. & Boone, C. (1997). Bni1p, a yeast formin linking cdc42p and the actin cytoskeleton during polarized morphogenesis. *Science,* **276**, 118-122.

Fedorov, A. A., Magnus, K. A., Graupe, M. H., Lattman, E. E., Pollard, T. D. & Almo, S. C. (1994a). X-ray structures of isoforms of the actin-binding protein profilin that differ in their affinity for phosphatidylinositol phosphates. *Proc. Natl Acad. Sci. USA,* **91**, 8636-8640.

Fedorov, A. A., Pollard, T. D. & Almo, S. C. (1994b). Purification, characterization and crystallization of human platelet profilin expressed in *Escherichia coli*. *J. Mol. Biol.* **241**, 480-482.

Fedorov, A. A., Ball, T., Mahoney, N., Valenta, R. & Almo, S. C. (1997). The molecular basis for allergen cross-reactivity: crystal structure and IgE-epitope mapping of birch pollen profilin. *Structure,* **5**, 33-45.

Finkel, T., Theriot, J. A., Dise, K. R., Tomaselli, G. F. & Goldschmidt-Clermont, P. J. (1994). Dynamic actin structures stabilized by profilin. *Proc. Natl Acad. Sci. USA,* **91**, 1510-1514.

Gertler, F. B., Niebuhr, K., Reinhard, M., Wehland, J. & Soriano, P. (1996). Mena, a relative of VASP and *Drosophila* enabled, is implicated in the control of the microfilament dynamics. *Cell,* **87**, 227-239.

Gieselmann, R., Kwiatkowski, D. J., Janmey, P. A. & Witke, W. (1995). Distinct biochemical characteristics of the two human profilin isoforms. *Eur. J. Biochem.* **229**, 621-628.

Goldschmidt-Clermont, P. J., Machesky, L. M., Baldassare, J. J. & Pollard, T. D. (1990). The actin-binding protein profilin binds to PIP_2 and inhibits its hydrolysis by phospholipase C. *Science,* **247**, 1575-1578.

Goldschmidt-Clermont, P. J., Kim, J. W., Machesky, L. M., Rhee, S. G. & Pollard, T. D. (1991a). Regulation of phospholipases C-γ1 by profilin and tyrosine phosphorylation. *Science,* **251**, 1231-1233.

Goldschmidt-Clermont, P. J., Machesky, L. M., Doberstein, S. K. & Pollard, T. D. (1991b). Mechanism of interaction of human platelet profilin with actin. *J. Cell. Biol.* **113**, 1081-1089.

Haarer, B. K., Petzold, A. S. & Brown, S. S. (1993). Mutational analysis of yeast profilin. *Mol. Cell. Biol.* **13**, 7864-7873.

Honoré, B., Madsen, P., Andersen, A. H. & Leffers, H. (1993). Cloning and expression of a novel human profilin variant, profilin II. *FEBS Letters,* **330**, 151-155.

Hutchinson, E. G. & Thornton, J. M. (1996). PROMOTIF - a program to identify and analyze structural motifs in proteins. *Protein Sci.* **5**, 212-220.

Janin, J. & Chothia, C. (1978). Role of hydrophobicity in the binding of coenzymes. *Biochemistry,* **17**, 2943-2948.

Johnson, B. H. & Hecht, M. H. (1994). Recombinant proteins can be isolated from *E. coli* cells by repeated cycles of freezing and thawing. *Biotechnology,* **12**, 1357-1360.

Jonckheere, V., Lambrechts, A., Vanderkerckhove, J. & Ampe, C. (1999). Dimerization of profilin II upon binding the $(GP_5)_3$ peptide from VASP overcomes the inhibition of actin nucleation by profilin II and thymosin β4. *FEBS Letters,* **447**, 257-263.

Jones, T. A., Zou, J.-Y., Cowtan, S. W. & Kjeldgaard, M. (1991). Improved methods for building protein models in electron density maps and the location of errors in these models. *Acta Crystallog. sect. A,* **47**, 110-119.

Korenbaum, E., Nordberg, P., Björkegren-Sjögren, C., Schutt, C. E., Lindberg, U. & Karlsson, R. (1998). The role of profilin in actin polymerization and nucleotide exchange. *Biochemistry,* **37**, 9274-9283.

Kwiatkowski, D. J. & Bruns, G. A. P. (1988). Human profilin: molecular cloning, sequence comparison, and chromosomal analysis. *J. Biol. Chem.* **263**, 5910-5915.

Lambrechts, A., van Damme, J., Goethals, M., Vanderkerckhove, J. & Ampe, C. (1995). Purification and characterization of bovine profilin II: actin, poly(L-proline) and inositolphospholipid binding. *FEBS Letters,* **230**, 281-286.

Lambrechts, A., Verschelde, J. L., Jonckheere, V., Goethals, M., Vanderkerchove, J. & Ampe, C. (1997). The mammalian profilin isoforms display complementary affinities for PIP_2 and proline-rich sequences. *EMBO J.* **16**, 484-494.

Lassing, I. & Lindberg, U. (1985). Specific interaction between phosphatidylinositol 4,5-bisphosphate and the profilin:actin complex. *Nature,* **314**, 472-474.

Lee, C.-H., Leung, B., Lemmon, M. A., Zheng, J., Cowburn, D., Kuriyan, J. & Saksela, K. (1995). A single amino acid in the SH3 domain of hck determines its high affinity and specificity in binding to HIV-1 nef protein. *EMBO J.* **14**, 5006-5015.

Lee, C.-H., Saksela, K., Mirza, U. A., Chait, B. T. & Kuriyan, J. (1996). Crystal structure of the conserved core of HIV-1 nef complexed with a src family SH3 domain. *Cell,* **85**, 931-942.

Lim, W. A. (1996). Reading between the lines: SH3 recognition of an intact protein. *Structure,* **4**, 657-659.

Lindberg, U., Schutt, C. E., Hellsten, E., Tjäder, A. C. & Hult, T. (1988). The use of poly(L-proline)-Sepharose in the isolation of profilin and profilactin complexes. *Biochim. Biophys. Acta,* **967**, 391-400.

Lu, P.-J., Shieh, W. R., Rhee, S. G., Yin, H. L. & Chen, C. S. (1996). Lipid products of phosphoinositide 3-kinase bind human profilin with high affinity. *Biochemistry,* **35**, 14027-14034.

Lynch, E. D., Lee, M. K., Morrow, J. E., Welcsh, P. L., Leon, P. E. & King, M.-C. (1997). Nonsyndromic deafness DFNA1 associated with mutation of a human homolog of the *Drosophila* gene *diaphanous*. *Science,* **278**, 1315-1318.

Mahoney, N. M., Janmey, P. A. & Almo, S. C. (1997). Structure of the profilin- poly-L-proline complex involved in morphogenesis and cytoskeletal regulation. *Nature Struct. Biol.* **4**, 953-960.

Mahoney, N. M., Rozwarski, D. A., Fedorov, E., Fedorov, A. A. & Almo, S. C. (1999). Profilin binds proline-rich ligands in two distinct amide backbone orientations. *Nature Struct. Biol.* **6**, 666-671.

Mammato, A., Sasaki, T., Asakura, T., Hotta, I., Imamura, H., Takahashi, K., Matsuura, Y., Shirao, T. & Takai, Y. (1998). Interactions of drebrin and gephyrin with profilin. *Biochem. Biophys. Res. Commun.* **243**, 86-89.

Manseau, L., Calley, J. & Phan, H. (1996). Profilin is required for posterior patterning of the *Drosophila* oocyte. *Development,* **122**, 2109-2116.

McGaughey, G. B., Gagne, M. & Rappe, A. K. (1998). Π-stacking interactions: Alive and well in proteins. *J. Biol. Chem.* **273**, 15458-15463.

Metzler, W. J., Constantine, K. L., Friedrichs, M. S., Bell, A. J., Ernst, E. G., Lavoie, T. B. & Mueller, L. (1993). Characterization of the three-dimensional solution structure of human profilin:^{1}H, ^{13}C, ^{15}N NMR assignments and global folding pattern. *Biochemistry,* **32**, 13818-13829.

Milner-White, E. J., Ross, B. M., Ismail, R., Belhadj-Mostefa, K. & Poet, R. (1988). One type of gamma-turn, rather than the other gives rise to chain-reversal in proteins. *J. Mol. Biol.* **204**, 777-782.

Mitchell, J. B. O., Nandi, L., McDonald, I. K., Thornton, J. & Price, S. (1994). Amino/aromatic interactions in proteins: is the evidence stacked against hydrogen bonding? *J. Mol. Biol.* **239**, 315-331.

Mockrin, S. C. & Korn, E. D. (1980). *Acanthamoeba* profilin interacts with G-actin to increase the rate of exchange of actin-bound adenosine 5′-triphosphate. *Biochemistry,* **19**, 5359-5362.

Navaza, J. (1994). AMoRe: an automated package for molecular replacement. *Acta Crystallog. sect. A,* **50**, 157-167.

Nicholls, A., Sharp, K. A. & Honig, B. (1991). Protein folding and association: insights from the interfacial and thermodynamic properties of hydrocarbons. *Proteins: Struct. Funct. Genet.* **11**, 281-296.

Nishida, E. (1985). Opposite effects of cofilin and profilin from porcine brain on rate of exchange of actin-bound adenosine 5′-triphosphate. *Biochemistry,* **24**, 1160-1164.

Otwinowski, Z. & Minor, W. (1997). Processing of X-ray diffraction data collected in oscillation mode. *Methods Enzymol.* **276**, 307-326.

Pantaloni, D. & Carlier, M.-F. (1993). How profilin promotes actin filament assembly in the presence of thymosin β4. *Cell,* **75**, 1007-1014.

Perrin, D., Möller, K., Hanke, K. & Söling, H.-D. (1992). cAMP and Ca^{2+}-mediated secretion in parotid acinar cells is associated with reversible changes in the organization of the cytoskeleton. *J. Cell. Biol.* **116**, 127-134.

Pollard, T. D. & Cooper, J. A. (1984). Quantitative analysis of the effect of *Acanthamoeba* profilin on actin filament nucleation and elongation. *Biochemistry,* **23**, 6631-6641.

Pring, M., Weber, A. & Bubb, M. R. (1992). Profilin-actin complexes directly elongate actin filaments at the barbed end. *Biochemistry,* **31**, 1827-1836.

Raghunathan, V., Mowery, P., Rozycki, M., Lindberg, U. & Schutt, C. (1992). Structural changes in profilin accompany its binding to phosphatidylinositol 4,5-bisphosphate. *FEBS Letters,* **297**, 46-50.

Ramesh, N., Anton, I. M., Hartwig, J. H. & Geha, R. S. (1997). WIP, a protein associated with Wiskott-Aldrich syndrome protein, induces actin polymerization and redistribution in lymphoid cells. *Proc. Natl Acad. Sci. USA,* **94**, 14671-14676.

Reinhard, M., Giehl, K., Abel, K., Haffner, C., Jarchau, T., Hoppe, V., Jockusch, B. M. & Walter, U. (1995). The proline-rich focal adhesion and microfilament protein VASP is a ligand for profilins. *EMBO J.* **14**, 1583-1589.

Sanger, J. M., Mittal, B., Dome, J. S. & Sanger, J. W. (1989). Analysis of cell division using fluorescently labeled actin and myosin in living PtK2 cells. *Cell Motil. Cytoskel.* **14**, 201-219.

Schlüter, K., Schleicher, M. & Jockusch, B. M. (1998). Effects of single amino acid substitutions in the actin-binding on the biological activity of bovine profilin I. *J. Cell Sci.* **111**, 3261-3273.

Schutt, C. E., Myslik, J. C., Rozycki, M. D., Goonesekere, N. C. W. & Lindberg, U. (1993). The structure of crystalline profilin-β-actin. *Nature,* **365**, 810-816.

Singh, S. S., Chauhan, A., Murakami, N. & Chauhan, V. P. S. (1996). Profilin and gelsolin stimulate phosphatidylinositol 3-kinase activity. *Biochemistry,* **35**, 16544-16549.

Small, J. V. (1988). The actin cytoskeleton. *Electron Microsc. Rev.* **1**, 155-174.

Sohn, R. H., Chen, J., Koblan, K. S., Bray, P. F. & Goldschmidt-Clermont, P. J. (1995). Localization of a binding site for phosphatidylinositol. *J. Biol. Chem.* **270**, 21114-21120.

Stossel, T. P. (1993). On the crawling of animal cells. *Science,* **260**, 1086-1094.

Suetsugu, S., Miki, H. & Takenawa, T. (1998). The essential role of profilin in the assembly of actin for microspike formation. *EMBO J.* **17**, 6516-6526.

Thorn, K. S., Christensen, H. E., Shigeta, R., Huddler, D., Shalaby, L., Lindberg, U., Chua, N.-H. & Schutt, C. E. (1997). The crystal structure of a major allergen from plants. *Structure,* **5**, 19-32.

Verheyen, E. M. & Cooley, L. (1994). Profilin mutations disrupt multiple actin-dependent processes during *Drosophila* development. *Development,* **120**, 717-728.

Vinson, V. K., Archer, S. J., Lattman, E. E., Pollard, T. D. & Torchia, D. A. (1993). Three-dimensional solution structure of *Acanthamoeba* profilin-I. *J. Cell Biol.* **122**, 1277-1283.

Wasserman, S. (1998). FH proteins as cytoskeletal organizers. *Trends Cell Biol.* **8**, 111-115.

Watanabe, N., Madaule, P., Reid, T., Ischizaki, T., Watanabe, G., Kakizuka, A., Saito, Y., Nakao, K., Jockusch, B. M. & Narumiya, S. (1997). p140mDia, a mammalian homolog of *Drosophila* diaphanous, is a target protein for rho small GTPase and is a ligand for profilin. *EMBO J.* **16**, 3044-3056.

Widada, J. S., Ferraz, C. & Liautard, J. P. (1989). Total coding sequence of profilin cDNA from *Mus musculus* macrophage. *Nucl. Acids Res.* **17**, 2855.

Wills, Z., Marr, L., Goodman, C. & Van Vactor, D. (1999). Profilin and abl tyrosine kinase are required for motor axon outgrowth. *Neuron,* **22**, 291-299.

Witke, W., Sharpe, A. H. & Kwiatkowski, D. J. (1993). Profilin deficient mice are not viable. *Mol. Cell Biol.* **4**, 149a.

Witke, W., Podtelejnikov, A. V., Di Nardo, A., Sutherland, J. D., Gurniak, C. B., Dotti, C. & Mann, M. (1998). In mouse brain profilin I and profilin II associate with regulators of the endocytic pathway and actin assembly. *EMBO J.* **17**, 967-976.

Edited by R. Huber

(Received 27 July 1999; received in revised form 13 October 1999; accepted 13 October 1999)